

## SUPPLEMENTARY INFORMATION

**Supplementary Table 1. Key Resources.**

REAGENT or RESOURCE	SOURCE	IDENTIFIER
<b>Antibodies</b>		
Goat anti-OCT4	Santa Cruz	sc-8628 RRID:AB_653551
Rabbit anti-SOX2	Abcam	ab97959 RRID:AB_2341193
Goat anti-NANOG	R&D Systems	AF1997 RRID:AB_355097
Mouse anti-SSEA4	STEMCELL Technologies	60062AD RRID:AB_2721031
Mouse anti-TRA-1-60	STEMCELL Technologies	60064AD RRID:AB_2686905
Mouse anti-ACTB ( $\beta$ -actin)	Cell Signaling Technology	3700S RRID:AB_2242334
Rat anti-C-peptide	Developmental Studies Hybridoma Bank	GN-ID4 RRID:AB_2255626
Mouse anti-GATA4	Thermo Fisher Scientific	MA5-15532 RRID:AB_10989032
Rabbit anti-GLUT2	Abcam	ab95256 RRID:AB_10859605
Rabbit anti-GLUT2	Santa Cruz	sc-9117 RRID:AB_641068
Rabbit anti-HNF1A	Abcam	ab96777 RRID:AB_10679303
Goat anti-HNF1A	Santa Cruz	sc-6547 RRID:AB_648295
Goat anti-HNF1A	Santa Cruz	sc-6548 RRID:AB_648293
Rabbit anti-HNF1A	Abcam	ab204306
Guinea pig anti-INS	Abcam	ab7842 RRID:AB_306130
Goat anti-NKX6.1	LifeSpan BioSciences	LS-C124275 RRID:AB_10805839
Guinea pig anti-PDX1	Abcam	ab47308 RRID:AB_777178
Goat anti-PDX1	R&D Systems	AF2419 RRID:AB_355257
<b>Chemicals, Peptides, and Recombinant Proteins</b>		
Dulbecco's High Glucose Modified Eagles Medium	HyClone™	#SH30022FS
DMEM medium with no glucose	Gibco™	11966025
DMEM/F12 with GlutaMAX supplement, Pyruvate	Invitrogen	10565042
GE Healthcare Fetal Bovine Serum	HyClone™	11521851
KnockOut Serum Replacement (KOSR)	Invitrogen	10828028
BSA	Sigma-Aldrich	A9418

<b>REAGENT or RESOURCE</b>	<b>SOURCE</b>	<b>IDENTIFIER</b>
GlutaMAX™ Supplement	Gibco™	11574466
Non-essential amino acids (NEAA)	Invitrogen	11140050
Beta-mercaptoethanol (1000X)	Gibco™	21985023
Trypsin-EDTA 0.25%	Gibco™	25300054
ReLeSR™	STEMCELL Technologies	05873
TrypLE™ Express Enzyme	ThermoFisher	12605010
Fibronectin	Sigma-Aldrich	F0895
Fisetin	MERCK	F4043
ECM	Sigma-Aldrich	E1270
D-Glucose	Sigma-Aldrich	G8769
Gelatin	MERCK	ES-006-B
Glibenclamide	Sigma-Aldrich	G0639
Ionomycin calcium salt	Sigma-Aldrich	I0634
L-Ascorbic acid (vitamin C)	Sigma-Aldrich	A92902
Penicilin/Streptomycin	Gibco™	15140122
Potassium Chloride	Merck	7447-40-7
Y-27632	STEMCELL Technologies	72302
FGF2	MACS	130-093-840
Activin A	R&D Systems	338-AC-50
CHIR-99021	Tocris	4423
BMP4	STEMCELL Technologies	02524
SB431542	Abcam	AB120163
FGF7	MACS	130-097-178
SANT-1	Santa Cruz	sc-203253
LDN193189	Sigma	SML0559-5MG
RA	Sigma	D2650-10
LY294002	LC Labs	L-7962
LDN	Stemgent	04-0019
ITS-X	Thermo Fisher Scientific	51500-056
PDBu	Tocris	4153
T3	Millipore	642511

REAGENT or RESOURCE	SOURCE	IDENTIFIER
ALK5 inhibitor II	Enzo Life Sciences	ALX-270-445
Heparin	Sigma-Aldrich	H3149
Transferrin	Sigma-Aldrich	T8158-100MG
Sodium selenite	Sigma-Aldrich	214485-100G
hBTC	Cell Signaling Technologies	5235SF
XXI	Millipore	565790
<b>Commercial Assays</b>		
Nucleospin® RNA kit	Macherey-Nagels	740955.250
iTaq™ Universal SYBR® Green Supermix	Bio-Rad Laboratories	1725125
High-Capacity cDNA Reverse Transcription Kit	Applied Biosystems	4368814
Glucose Uptake Colorimetric Assay Kit	Sigma-Aldrich	MAK083
ADP/ATP Bioluminescence Assay Kit (ApoSENSOR)	Biovision Incorporated	K255
Mercodia Insulin ELISA	Mercodia Immunoassays and Services	10-1113-01
C-peptide ELISA	Mercodia	10-1136-01
Dual Luciferase Assay System	Promega	E1980
<b>Deposited Data</b>		
RNA-sequencing	This paper	GSE140208
ChIP-sequencing	This paper	GSE139832
<b>Experimental Models: Cell Lines</b>		
H9 hESC line	WiCell Research Institute	NIHhESC-10-0062 RRID:CVCL_9773
AD-293 line	Agilent	240085 RRID:CVCL_KA63
EndoC-βH1 line	Univercell Biosolutions	EndoC-βH1 RRID:CVCL_L909
Fibroblast (to generate iAGb)	Coriell Institute	AG16102 RRID:CVCL_2G48
CF-1 MEF	Gibco	A34181 RRID:CVCL_5251
<b>Experimental Models: Organisms/Strains</b>		
NOD-SCID mice	Taconic Biosciences	NOD/MrkBomTac- <i>Prkdc</i> <sup>scid</sup> RRID:IMSR_TAC:nodsc
<b>Software and Algorithms</b>		

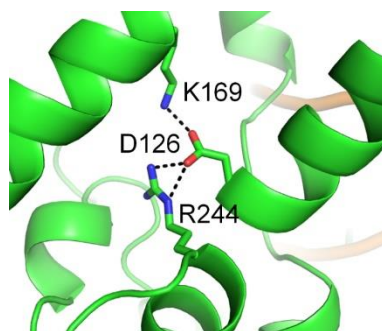
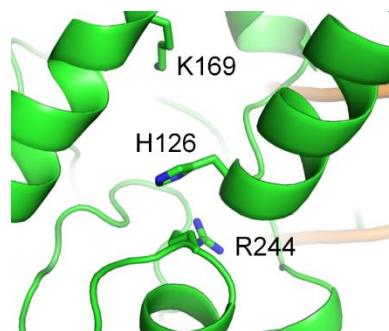
<b>REAGENT or RESOURCE</b>	<b>SOURCE</b>	<b>IDENTIFIER</b>
PRISM v8 graphing and statistical software	GraphPad	<a href="http://www.graphpad.com/scientific-software/prism/">http://www.graphpad.com/scientific-software/prism/</a> RRID:SCR_002798
FlowJo 7.0 software	BD Biosciences	<a href="https://www.flowjo.com/solutions/flowjo/">https://www.flowjo.com/solutions/flowjo/</a> RRID:SCR_008520

**Supplementary Table 2. Quantitative real-time PCR primers used in this study.**

<b>Gene</b>	<b>Accession Number</b>	<b>Forward Primer (5' to 3')</b>	<b>Reverse Primer (5' to 3')</b>
<i>ABHD15</i>	NM_198147	GCTGTTCGCGGTGAGCGAAG	GGCATACCTGCTGAGGGCGAT
<i>ACTB</i>	NM_001101	TTGCCGATCCGCCGCCCGTC	CCCATGCCACCATCACGCCCTG
<i>ANKS4B</i>	NM_145865	TGGCCAAGTTCTGGTGAGCAGG	GGGTCCCCTCCTCTACTGCAGATT
<i>FGFR4</i>	NM_002011	GGAGCGCTCGGGCTGTCTG	TGCCTTCCTGGCTCCTCCTCA
<i>GLIS3</i>	NM_001042413	CGGACGCATCTGGACACCAAAC	GGGACTGCACGGTGAGGCAA
<i>GLUT1</i>	NM_006516	AGCAGCAAGAAGCTGACGGGTCGCC	AGCGTGGTGAGCGTGGTGGGC
<i>GLUT2</i>	NM_000340	TTGGTGGGTGGCTTGGGGAC	ACCAGGCCTGAAATTAGCCCACA
<i>GLUT3</i>	NM_006931	GCTAAGCAGATCCTCCAGCGGT	ATTAACCACACCCGCGCCGA
<i>GPR39</i>	NM_001508	GCAGACCATCATCTTCCTGAGGCT	GTCGTGCTTGGGTTTGGCCG
<i>HNF1A</i>	NM_001306179	CTTCTGCAGGAGGACCCGTGGCGT	GGCGGCCCGCTTCTGCGTCT
<i>HNF4A</i>	NM_178849	GGACGACCAGGTGGCCCTGCTCAGA	GCTCCGGGCAGTGCCGAGGGA
<i>INS</i>	NM_000207	CCTGCAGGTGGGGCAGGTGGAGC	CGGGTGTGGGGCTGCCTGCG
<i>LAMA1</i>	NM_005559	ACAGCGCAAACCCAGAGAACGCCA	CCAGGTCGAGGGGCATTGGCAGC
<i>NRARP</i>	NM_001004354	TGGGTGGAGTTTGTGCGCCT	CACCATCAGGCTGGGCGGTA
<i>PAK4</i>	NM_005884	AGTTAGGCCGCGAGCGACTG	GTGCGGCCTGGTCTGATGCT
<i>PDGFA</i>	NM_002607	CGGGCCGCGCTCCCTAAG	CGGCTTCCTCGGCCAGAACA
<i>TM4SF4</i>	NM_004617	CGATTTGCGATGTTACCTCCACG	GAGGCTCTCGGCACTTGTTCCA
<i>TSPAN8</i>	NM_004616	AGTCGCTGCATGCTTCTGTTGTTTT	CCCCTGTGGCGCTCAAAGC
<i>UGT2B4</i>	NM_021139	TGCCAAACCCCTACCGAAGGAAA	TGTGGGATCTTGGCAAGGGCT

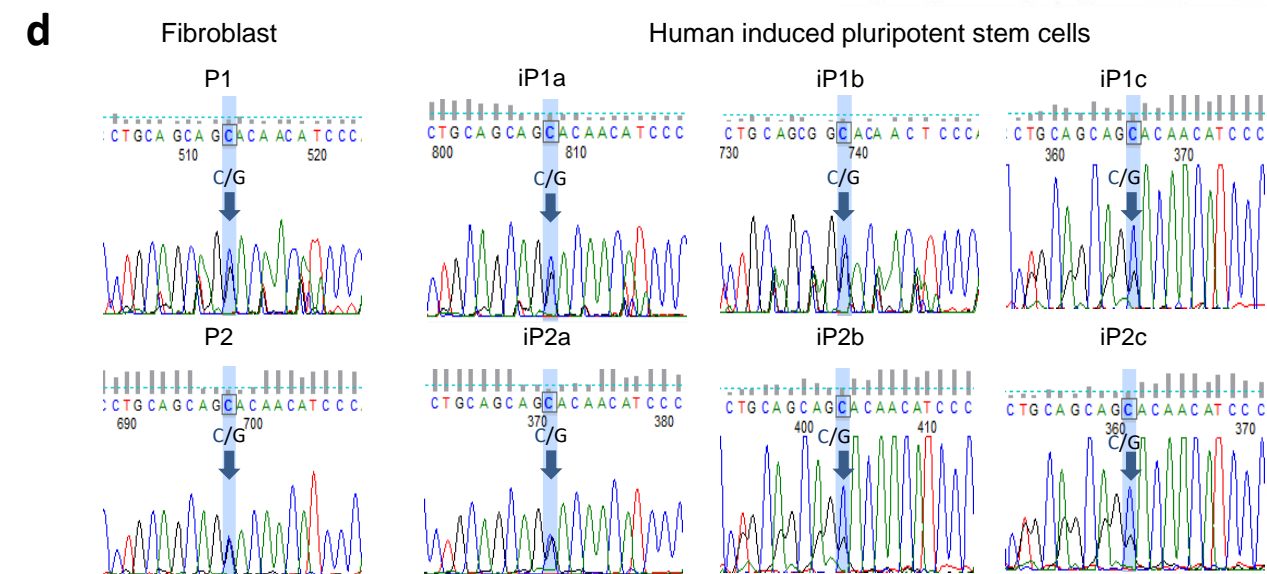
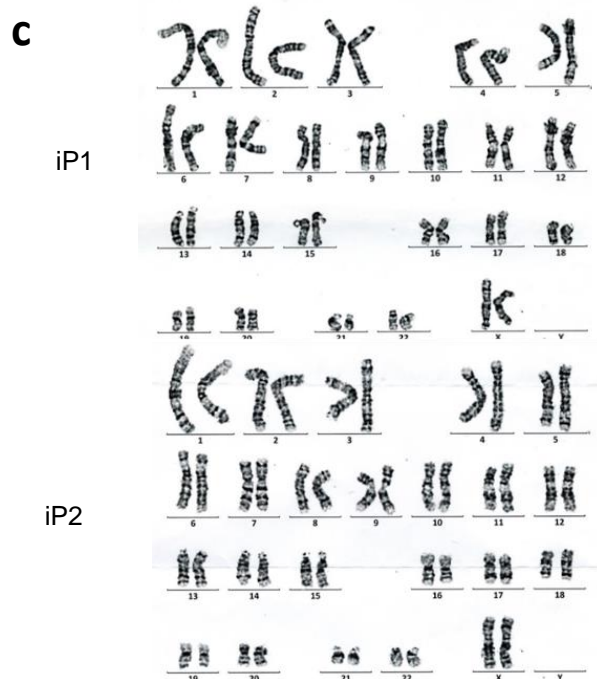
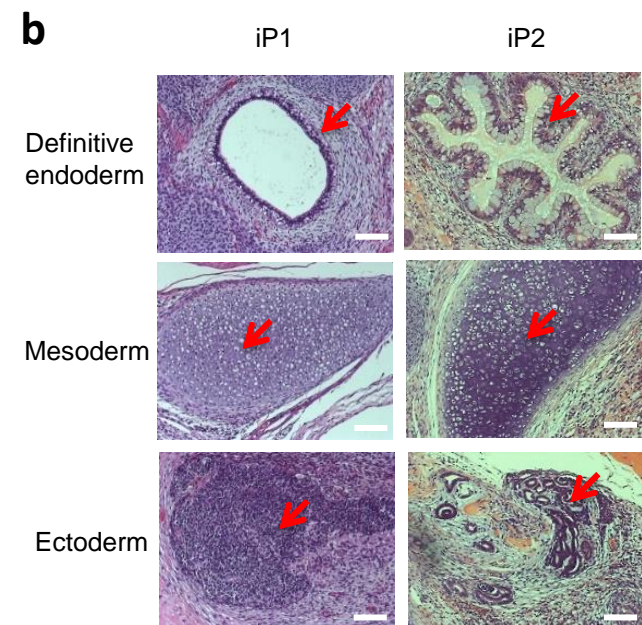
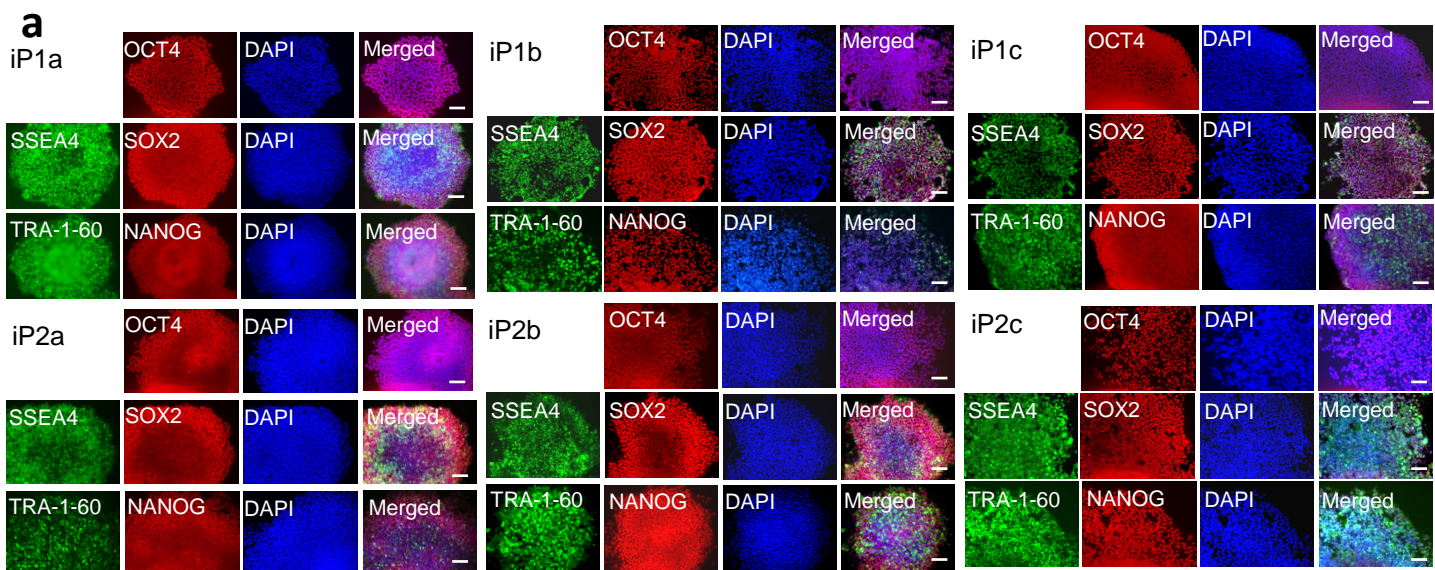
Figure S1: Low et al.,

a



**Supplementary Figure 1. Interactions of residue 126 in HNF1A–DNA complex.** Crystal structure of WT HNF1A–DNA complex (PDB 1IC8) (Chi et al., 2002). Final trajectory structure obtained from accelerated molecular dynamics (aMD) simulation of mutant HNF1A H126D–DNA complex.

Figure S2: Low et al.,

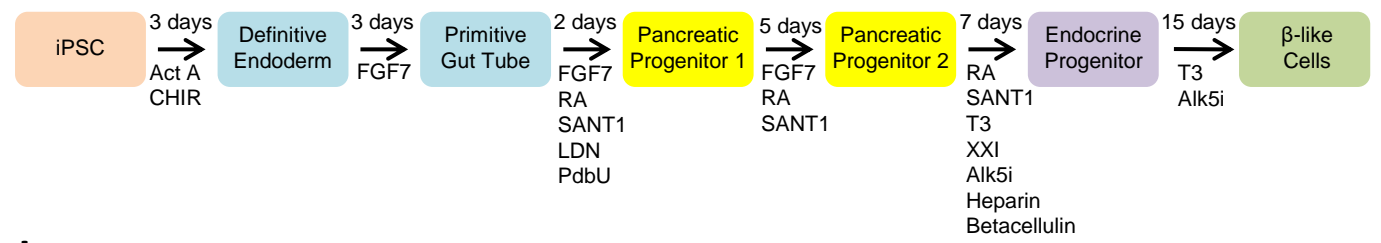


## Supplementary Figure 2. Characterization of MODY3-hiPSCs.

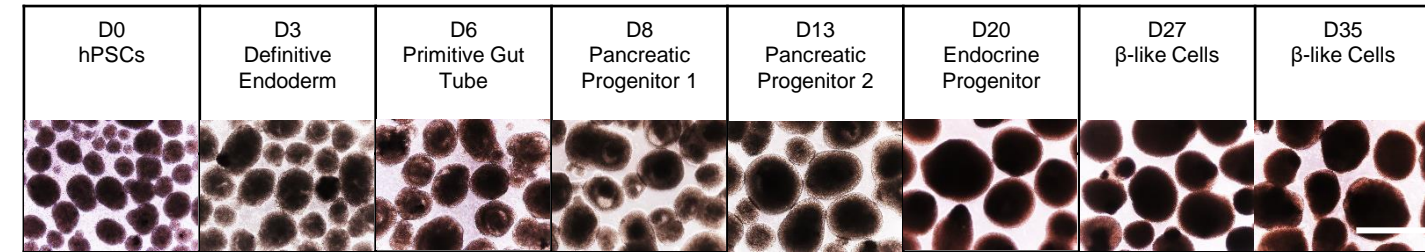
(a) Immunohistochemistry stain for pluripotency markers OCT4 (red), SOX2 (red), SSEA4 (green), NANOG (red) and TRA-1-60 (green) and nuclear stain using DAPI (blue). n = 3 independent experiments. (scale bar:100µM). (b) Hematoxylin and eosin (H&E) stain of teratoma tissue section formed by patient-derived hiPSCs. Presence of three germ layers (indicated by red arrows): definitive endoderm, mesoderm, ectoderm. n = 1 independent experiment. (scale bar: 100 µm). (c) Karyotyping analysis confirmed normal karyotype of hiPSCs derived from P1 and P2. (d) Cycle sequencing confirmed the presence of heterozygous *HNF1A*<sup>+/H126D</sup> mutation (highlighted) in patient-derived hiPSCs. Cytosine in blue, thymine in red, guanine in black, adenine in green. hiPSCs: human induced pluripotent stem cells. iP1a-c: hiPSC lines generated from P1, iP2a-c: hiPSC lines generated from P2. P1: patient 1, P2: patient 2.

# Figure S3: Low et al.,

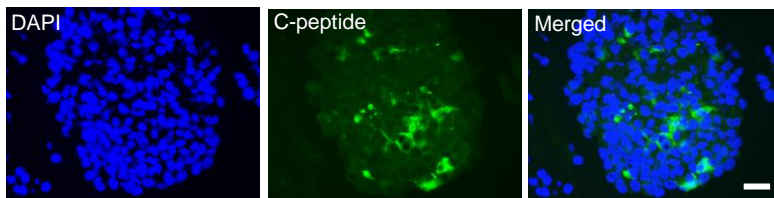
**a**



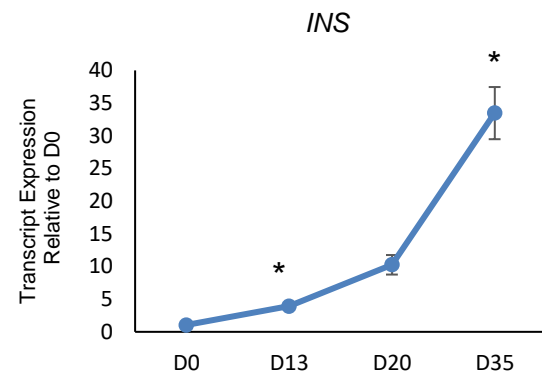
**b**



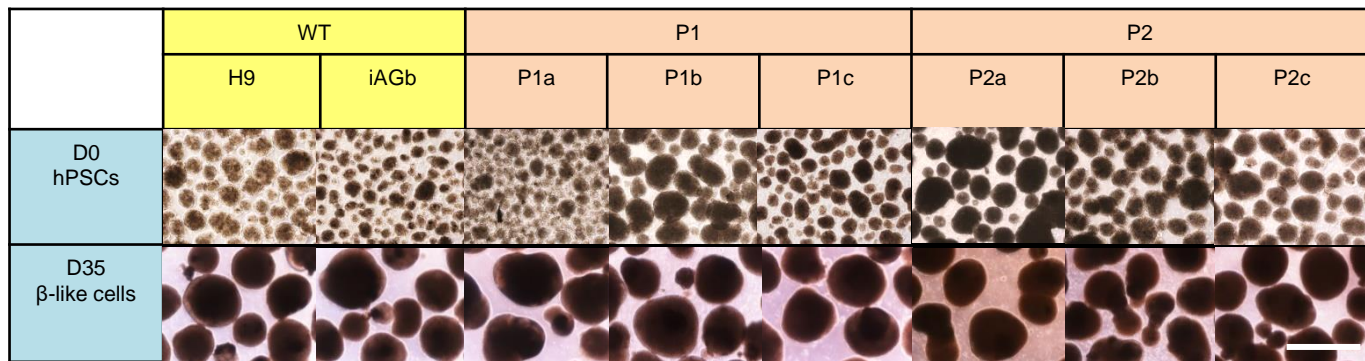
**c**



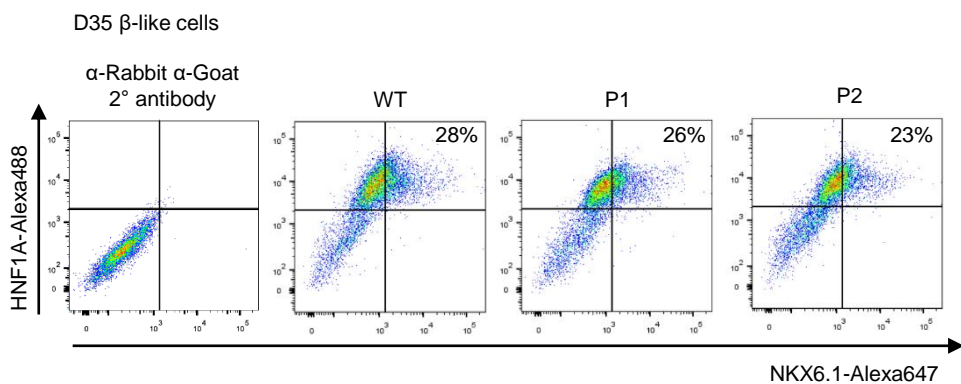
**d**



**e**

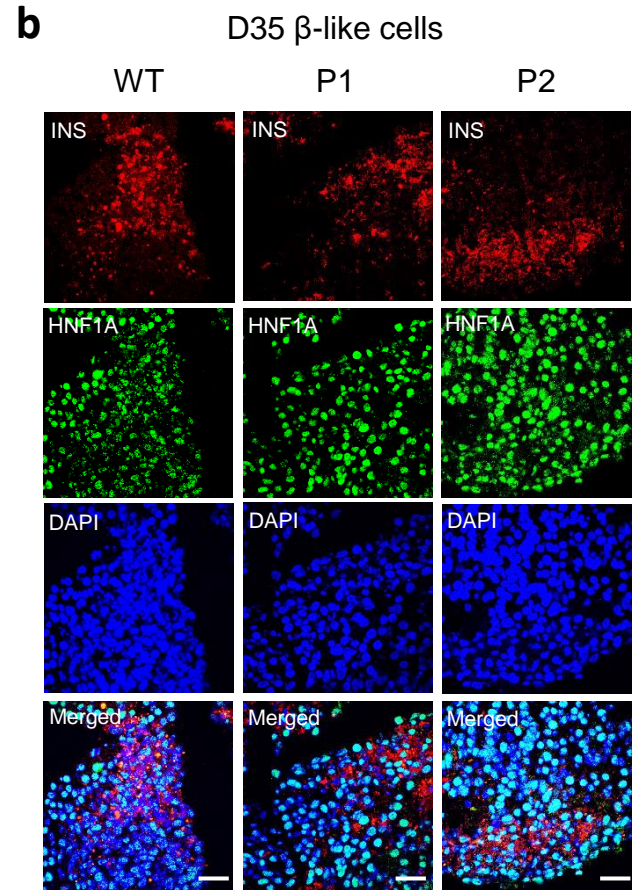
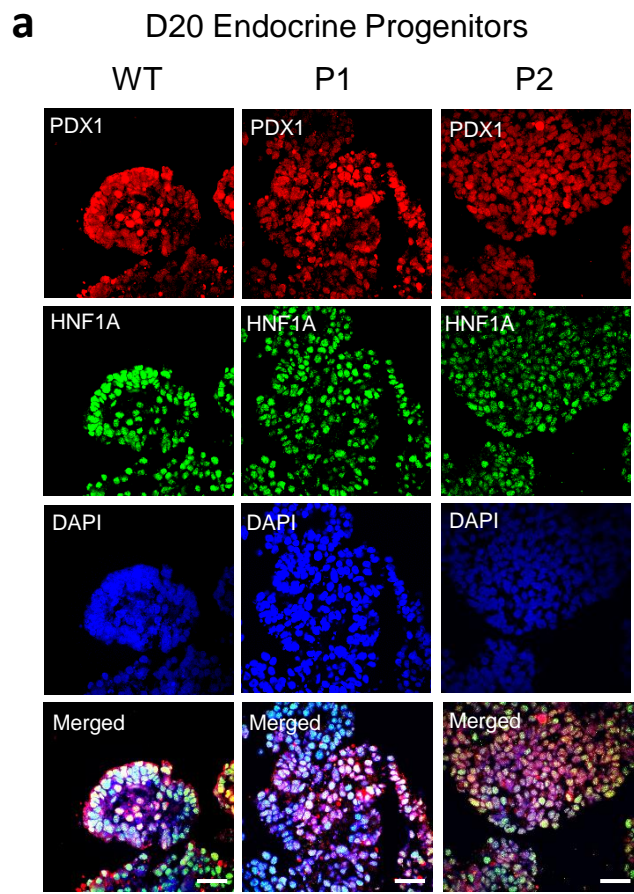


**f**



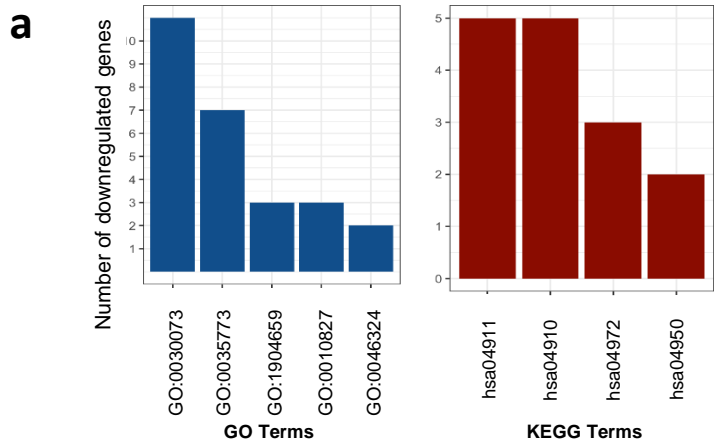
**Supplementary Figure 3. Differentiation of MODY3 patient-specific hiPSCs along the pancreatic lineage.** (a) Schematic of differentiation protocol and growth factors added at each stage of pancreatic differentiation. (b) Cell clusters at various stages during the 35-day pancreatic differentiation. n = 3 independent experiments. (scale bar: 100  $\mu$ m). (c) Immunohistochemistry stain for C-peptide protein (green) and nuclear stain using DAPI (blue) in H9 cell clusters at day 35 of pancreatic differentiation. n = 3 independent experiments. (scale bar: 50  $\mu$ m). (d) RT-qPCR analysis of *INS* transcripts in H9 during various stages of pancreatic differentiation. n = 3 independent experiment. Error bars represent standard error of mean (SEM). (e) WT and mutant cell clusters at the start and end of the 35-day pancreatic differentiation. n = 3 independent experiments. (scale bar: 100  $\mu$ m). (f) Flow cytometry analysis of HNF1A and NKX6.1 proteins in D35  $\beta$ -like cells. D: day of differentiation. hPSCs: human pluripotent stem cells. P1a-c: cell lines generated from P1, P2a-c: cell lines generated from P2. WT: wild type, P1: patient 1, P2: patient 2. For all statistical analysis: Error bars represent standard error of mean (SEM). Unpaired one-tailed Student's t-test was performed. \* indicates P-value < 0.05 compared to D0. Source data are provided as a Source data file.

Figure S4: Low et al.,



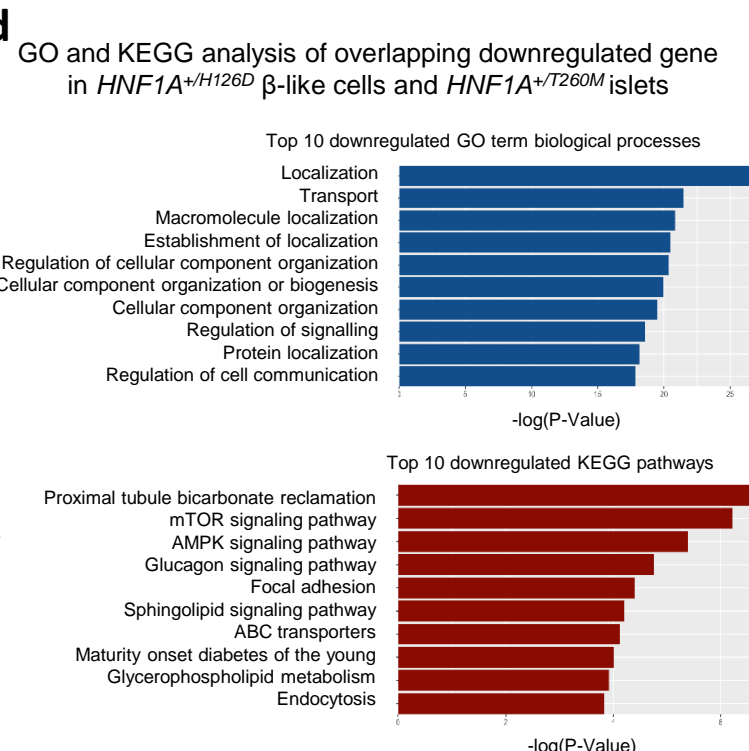
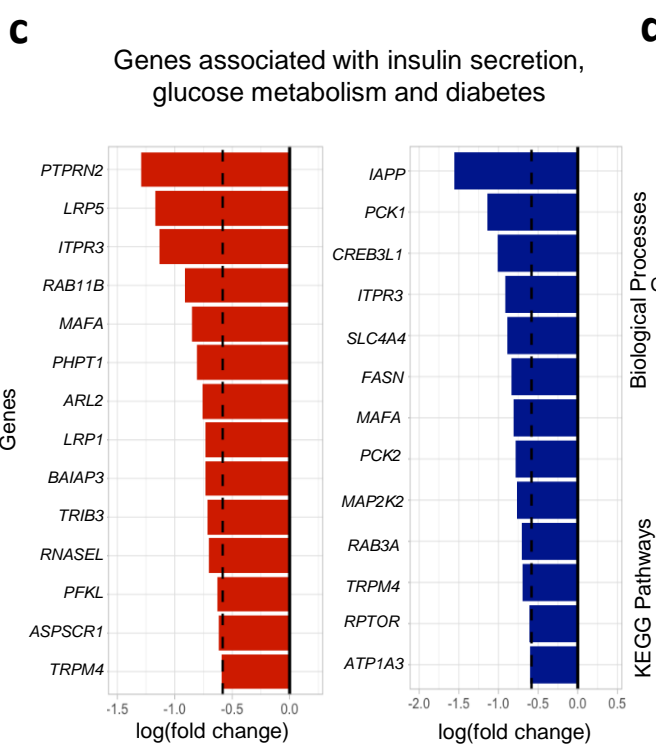
**Supplementary Figure 4. Comparison of pancreatic differentiation between WT and MODY3-hiPSCs.** (a) Immunohistochemistry stain for HNF1A protein (green), PDX1 protein (red) and nuclear stain using DAPI (blue) in WT, P1 and P2 endocrine progenitor cell clusters at day 20 of pancreatic differentiation. n = 3 independent experiments. (scale bar: 100  $\mu$ m). (b) Immunohistochemistry stain for HNF1A protein (green), INS protein (red) and nuclear stain using DAPI (blue) in WT, P1 and P2 D35  $\beta$ -like cell clusters at day 35 of pancreatic differentiation. n = 3 independent experiments. (scale bar: 100  $\mu$ m). D: day of differentiation. WT: wild type, P1: patient 1, P2: patient 2. hiPSCs: human induced pluripotent stem cells. Source data are provided as a Source data file.

Figure S5: Low et al.,



**b**

GO/KEGG ID	Description	Downregulated Genes	P-value
GO:0030073	insulin secretion	<i>PTPRN2, BAIAP3, LRP5, MAFA, PHPT1, LRP1, TRPM4, PFKL, RAB11B, ARL2, ITPR3</i>	0.002
GO:0035773	insulin secretion involved in cellular response to glucose stimulus	<i>PTPRN2, BAIAP3, LRP5, PHPT1, LRP1, TRPM4, RAB11B</i>	0.012
GO:1904659	glucose transmembrane transport	<i>RNASEL, TRIB3, ASPSCR1</i>	0.214
GO:0010827	regulation of glucose transmembrane transport	<i>RNASEL, TRIB3, ASPSCR1</i>	0.295
GO:0046324	regulation of glucose import	<i>RNASEL, ASPSCR1</i>	0.512
hsa04911	Insulin secretion Pathway	<i>RAB3A, ATP1A3, TRPM4, CREB3L1, ITPR3</i>	0.177
hsa04910	Insulin signalling pathway	<i>RPTOR, MAP2K2, PCK1, PCK2, FASN</i>	0.353
hsa04972	Pancreatic secretion	<i>SLC4A4, ATP1A3, ITPR3</i>	0.042
hsa04950	Maturity onset diabetes of the young	<i>MAFA, IAPP</i>	0.060

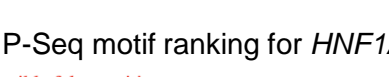


**Supplementary Figure 5. Bioinformatics analyses of *HNF1A* transcriptomics datasets.** (a) Number of gene candidates that are downregulated in *HNF1A*<sup>+/*H126D*</sup> endocrine progenitors that are associated with insulin secretion, glucose metabolism and diabetes according to Gene Ontology (GO) and Kyoto Encyclopedia of Genes and Genomes (KEGG) annotation. Unadjusted P-value were calculated using two-sided Mann-Whitney U test according to the GOSeq protocol (Young et al., 2010). (b) Table showing the details of each GO and KEGG annotation along with the list of gene candidates and P value. Unadjusted P-value were calculated using two-sided Mann-Whitney U test according to the GOSeq protocol (Young et al., 2010). (c) Transcript fold change of gene candidates that are downregulated in *HNF1A*<sup>+/*H126D*</sup> endocrine progenitors that are associated with insulin secretion, glucose metabolism and diabetes based on RNA-Seq analysis. Black dotted line indicates cut-off of 1.5-fold. (d) GO and KEGG analysis of the 347 genes commonly downregulated in both *HNF1A*<sup>+/*H126D*</sup> endocrine progenitors and *HNF1A*<sup>+/*T260M*</sup> islets. Bar chart showing the top 10 GO biological processes and KEGG pathway affected, ranked by ascending order of p value. Unadjusted P-value were calculated using two-sided Mann-Whitney U test according to the GOSeq protocol (Young et al., 2010). ChIP-Seq: Chromatin immunoprecipitation sequencing. WT: wild type.

Figure S6: Low et al.,

**a** CHIP-Seq motif ranking for WT endocrine progenitors

\* - possible false positive

Rank	Motif	P-value	log P-pvalue	% of Targets	% of Background
1		1e-229	-5.281e+02	57.38%	1.53%
2		1e-16	-3.773e+01	22.62%	7.34%
3		1e-13	-3.155e+01	2.30%	0.01%
4		1e-12	-2.884e+01	7.87%	1.14%
5		1e-12	-2.841e+01	5.57%	0.49%
6 *		1e-11	-2.665e+01	10.82%	2.49%
7 *		1e-10	-2.324e+01	1.64%	0.01%
8 *		1e-9	-2.267e+01	3.28%	0.16%
9 *		1e-9	-2.150e+01	24.59%	11.79%
10 *		1e-8	-2.015e+01	3.28%	0.21%
11 *		1e-8	-1.888e+01	5.90%	1.05%
12 *		1e-7	-1.701e+01	0.98%	0.00%
13 *		1e-1	-3.693e+00	0.33%	0.01%

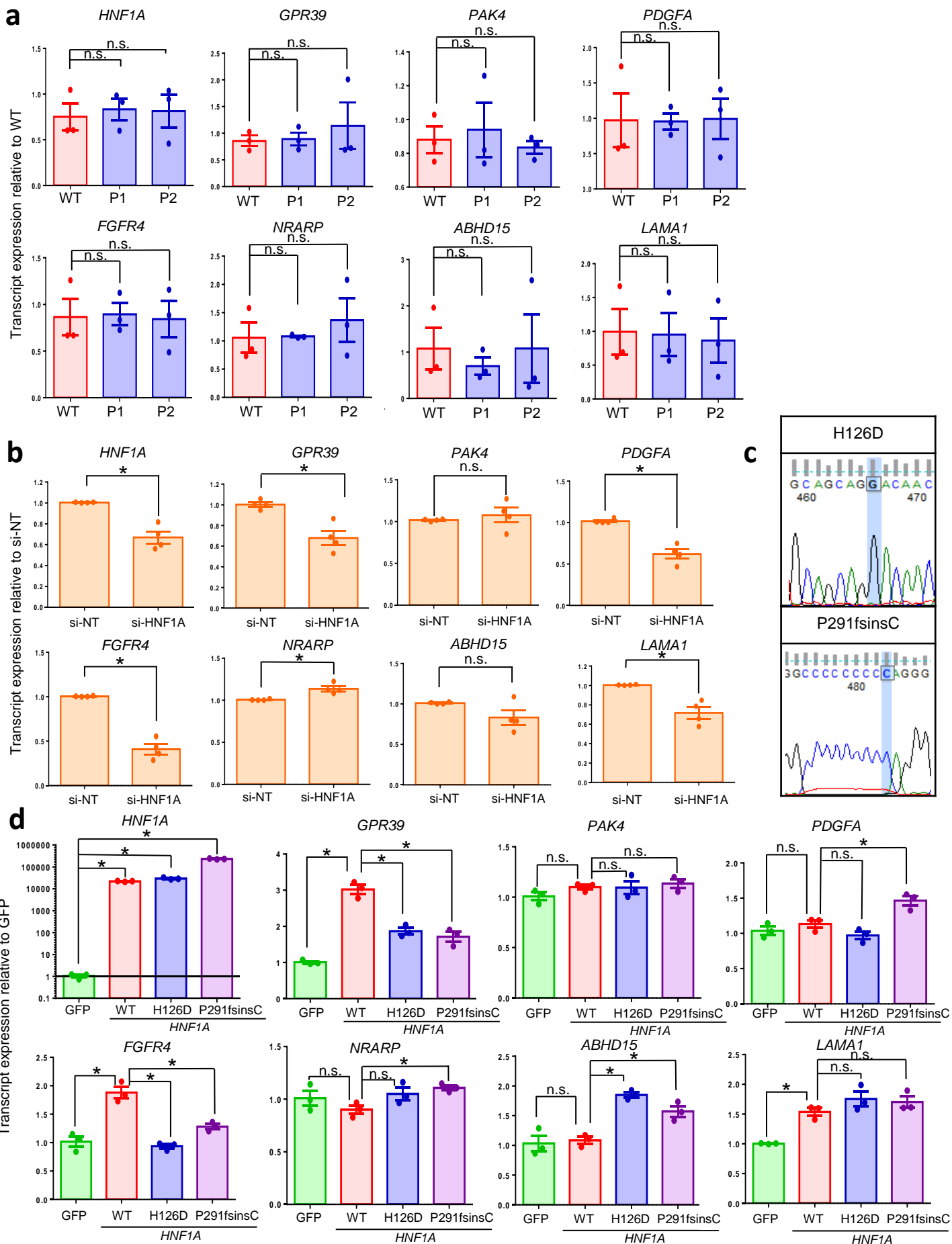
**b** CHIP-Seq motif ranking for *HNF1A*<sup>+H126D</sup> endocrine progenitors

\* - possible false positive

Rank	Motif	P-value	log P-pvalue	% of Targets	% of Background
1		1e-12	-2.782e+01	11.54%	0.06%
2 *		1e-10	-2.366e+01	23.08%	1.67%
3 *		1e-8	-2.033e+01	5.77%	0.00%
4 *		1e-8	-1.989e+01	7.69%	0.03%
5 *		1e-7	-1.736e+01	21.15%	2.34%
6 *		1e-7	-1.691e+01	15.38%	0.99%
7 *		1e-7	-1.652e+01	19.23%	1.98%
8 *		1e-6	-1.598e+01	11.54%	0.43%
9 *		1e-6	-1.444e+01	28.85%	6.37%
10 *		1e-4	-1.042e+01	19.23%	3.92%

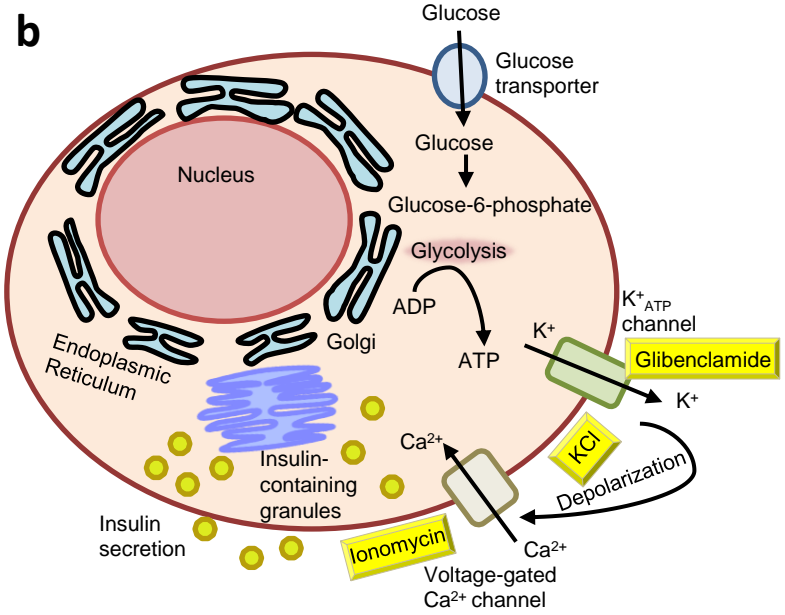
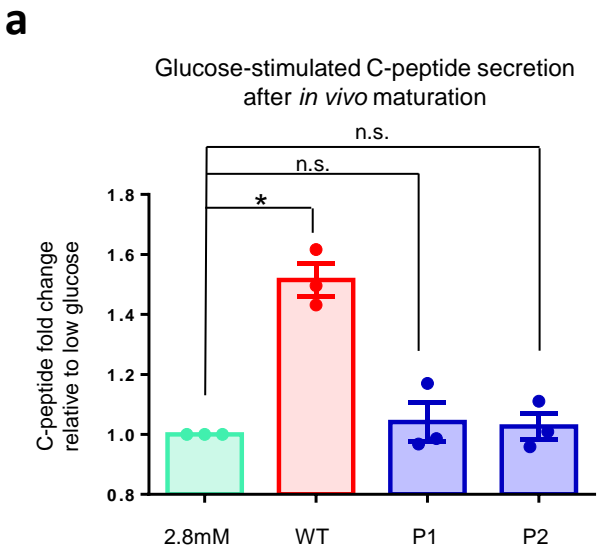
**Supplementary Figure 6. ChIP-Seq analyses of motifs enriched in the HNF1A-bound regions in WT and MODY3 endocrine progenitors.** Motifs enriched in the HNF1A-bound regions of (a) WT endocrine progenitors and (b) *HNF1A*<sup>+/*H126D*</sup> endocrine progenitors. Cumulative Poisson p-value was determined according to protocol specified in the HOMER software suite (v4.11) using findMotifsGenome.pl. (Heinz et al., 2010).

Figure S7: Low et al.,



**Supplementary Figure 7. Evaluation of putative HNF1A targets affected by *HNF1A*<sup>+/H126D</sup> mutation based on RNA-Seq and CHIP-Seq analyses.** RT-qPCR analysis of candidate genes in (a) WT (red) and mutant (blue) hPSC-derived endocrine progenitors. n = 3 independent experiments. or (b) EndoC-βH1 cells transfected with *HNF1A* siRNA (si-HNF1A) and non-targeting siRNA as negative control (si-NT). n = 3 independent experiments. P-value for *HNF1A* = 0.0102, *GPR39* = 0.0151, *PDGFA* = 0.0051, *FGFR4* = 0.0018, *NRARP* = 0.0220, *LAMA1* = 0.0180. (c) Cycle sequencing confirmed successful site directed mutagenesis nucleotide change (highlighted) to generate *HNF1A* constructs containing p.H126D c.376C>G and P291fsinsC mutations. Cytosine in blue, thymine in red, guanine in black, adenine in green. (d) RT-qPCR analysis of candidate genes in AD-293 cells overexpressed with GFP (green) and various WT (red), H126D (blue) and P291fsinsC (purple) *HNF1A* constructs. n = 3 independent experiments. P-value for *HNF1A* = 0.0007 (WT), 0.0034 (H126D), 0.0006 (P291fsinsC); *GPR39* = 0.0025 (WT), 0.0028 (H126D), 0.0023 (P291fsinsC); *PDGFA* = 0.0229 (P291fsinsC); *FGFR4* = 0.0034 (WT), 0.0056 (H126D), 0.0155 (P291fsinsC); *NRARP* = 0.0178 (P291fsinsC); *ABHD15* = 0.0007 (H126D), 0.01580 (P291fsinsC); *LAMA1* = 0.0141 (WT). GFP: green fluorescent protein. WT: wild type, P1: patient 1, P2: patient 2. RT-qPCR: quantitative reverse transcription polymerase chain reaction. hPSCs: human pluripotent stem cells. WT: wild type, P1: patient 1, P2: patient 2. For all statistical analysis: Error bars represent standard error of mean (SEM). Unpaired one-tailed Student's t-test was performed. \* indicates P-value < 0.05. Source data are provided as a Source data file.

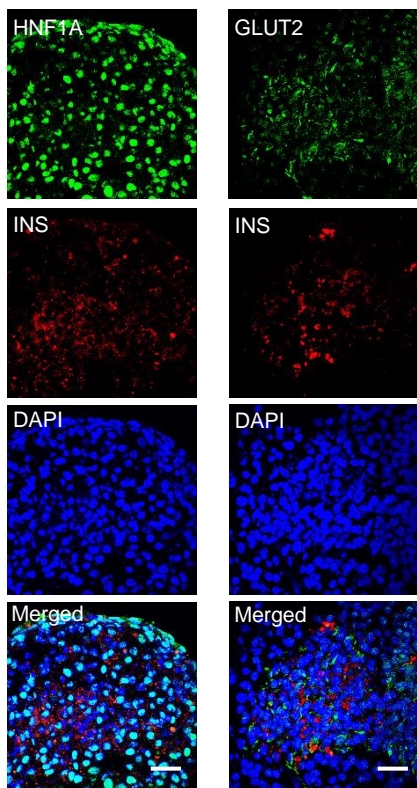
Figure S8: Low et al.,



**Supplementary Figure 8. Stimulus-secretion coupling in  $\beta$  cell.** (a) Glucose-stimulated C-peptide secretion of WT (red) and patient-specific (blue) hPSC-derived  $\beta$ -like cells after *in vivo* maturation in mouse kidney capsule for 23 weeks. All C-peptide fold changes are normalized to C-peptide amounts secreted at 2.8 mM glucose (green) under each condition.  $n = 3$  independent experiments;  $p = 0.0006$  (WT). (b) Diagram of stimulus-secretion coupling in human  $\beta$  cell. WT: wild type, P1: patient 1, P2: patient 2. hPSCs: human pluripotent stem cells. For all statistical analysis: Error bars represent standard error of mean (SEM). Unpaired one-tailed Student's t-test was performed. \* indicates P-value  $< 0.05$ . Source data are provided as a Source data file.

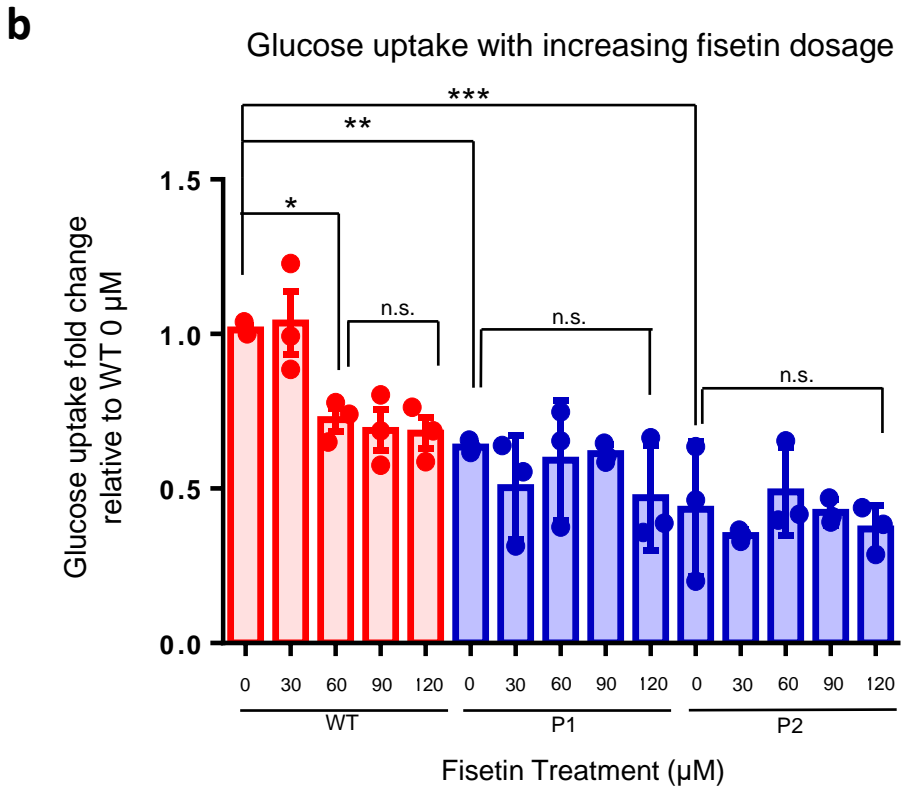
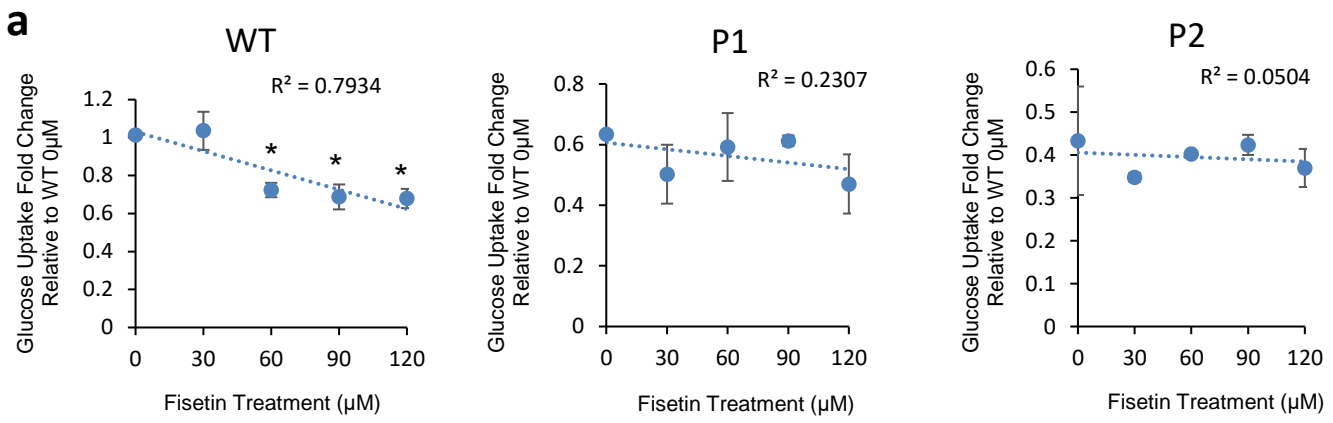
Figure S9: Low et al.,

a



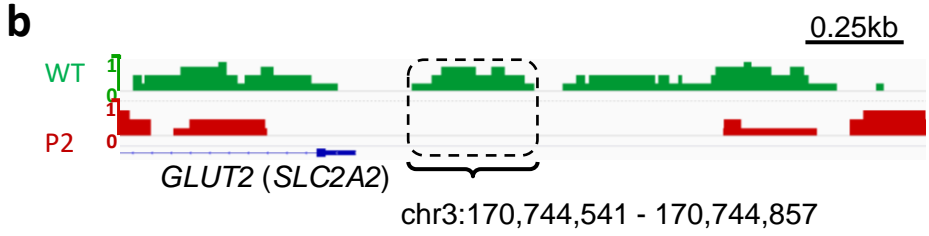
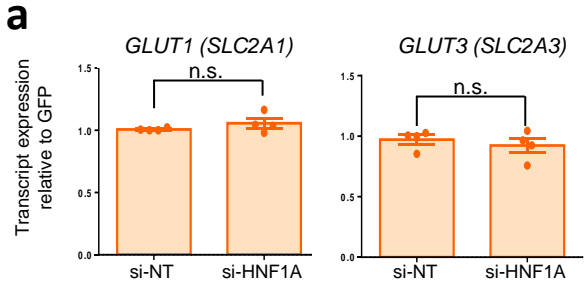
**Supplementary Figure 9. Evaluation of HNF1A and GLUT2 co-expression with INS in  $\beta$ -like cells.** Immunohistochemistry stain for HNF1A (green), GLUT2 (green), INS (red) proteins and nuclear stain using DAPI (blue) in cell clusters at day D35 of pancreatic differentiation. n = 3 independent experiments. (scale bar: 100  $\mu$ m). D: day of differentiation.

Figure S10: Low et al.,



**Supplementary Figure 10. Evaluation of increasing fisetin dosage on glucose uptake inhibition.** (a) Glucose uptake fold changes with increasing concentrations (0  $\mu\text{m}$ , 30  $\mu\text{m}$ , 60  $\mu\text{m}$ , 90  $\mu\text{m}$  and 120  $\mu\text{m}$ ) of GLUT2 inhibitor, fisetin in WT (red), P1 and P2 (blue) hPSC-derived  $\beta$ -like cells. Effectiveness of fisetin in reducing glucose uptake measured by Pearson's  $R^2$ . Glucose uptake fold changes are normalized to glucose uptake amount in the presence of dimethyl sulfoxide (DMSO) (0  $\mu\text{m}$  fisetin) in WT  $\beta$ -like cells.  $n = 3$  independent experiments;  $p = 0.0098$  (60  $\mu\text{m}$ ); 0.0341 (90  $\mu\text{m}$ ), 0.0172 (120  $\mu\text{m}$ ). \* indicates P-value  $< 0.05$  using pairwise t-test compared to 0  $\mu\text{m}$  treatment. (b) Glucose uptake in WT, P1 and P2 hPSC-derived  $\beta$ -like cells in the presence of DMSO (0  $\mu\text{m}$  fisetin) or increasing concentrations (30  $\mu\text{m}$ , 60  $\mu\text{m}$ , 90  $\mu\text{m}$  and 120  $\mu\text{m}$ ) of GLUT2 inhibitor, fisetin. Glucose uptake fold changes are normalized to glucose uptake amount in the presence of DMSO (0  $\mu\text{m}$  fisetin) in WT  $\beta$ -like cells.  $n = 3$  independent experiments. One-way ANOVA was performed for group comparison ( $p = 5.14 \times 10^{-7}$ , F-critical = 8.52). Pairwise t-test was performed for pairwise comparison among independent groups; \*  $p = 0.0098$ , \*\*  $p = 0.00003$ , \*\*\*  $p = 0.0429$ , n.s.: non-significant. WT: wild type, P1: patient 1, P2: patient 2. hPSCs: human pluripotent stem cells. For all statistical analysis: Error bars represent standard error of mean (SEM). Source data are provided as a Source data file.

Figure S11: Low et al.,



**Supplementary Figure 11. Evaluation of GLUTs.** (a) RT-qPCR analysis of *GLUT1* and *GLUT3* transcripts in EndoC- $\beta$ H1 cells transfected with *HNF1A* siRNA (si-HNF1A) and non-targeting siRNA as negative control (si-NT) (n=3). For all statistical analysis: Error bars represent standard error of mean (SEM). Unpaired one-tailed Student's t-test was performed. n = 3 independent experiments. \* indicates P-value < 0.05. (b) Histogram showing ChIP-Seq enrichment region in HNF1A-binding site on *GLUT2* (*SLC2A2*) promoter. Region where there is a difference in binding between WT (green) and P2 (*HNF1A*<sup>+H126D</sup>) (red) is highlighted in dotted-line box with the nearest coding gene shown. WT: wild type, P1: patient 1, P2: patient 2. RT-qPCR: quantitative reverse transcription polymerase chain reaction. ChIP-Seq: Chromatin immunoprecipitation sequencing. Source data are provided as a Source data file.